Kinetic Study of Heterogeneous Oxygen-Exchange Reactions and Bulk Self-Diffusion of Oxygen

Filip Acke* and Itai Panas

Department of Inorganic Chemistry, Chalmers University of Technology and Göteborg University, S-412 96 Göteborg, Sweden

Received: February 18, 1998; In Final Form: April 22, 1998

Apparent activation energies are determined for oxygen-isotope exchange reactions between O_2, CO, or NO and preoxidized or prereduced CaO surfaces. Oxygen exchange between $N^{16}O$ or $C^{16}O$ and isotope labeled $Ca^{18}O$ surfaces produced an apparent activation energy of 2 kcal/mol. Similar values are obtained for single-isotope-exchange between $^{18}O^{18}O$ and prereduced $Ca^{16}O$ surfaces. Apparent activation energies of 15−18 kcal/mol are found for single and double exchange between $^{18}O^{18}O$ and preoxidized $Ca^{16}O$ surfaces, as well as for double exchange between $^{18}O^{18}O$ and prereduced $Ca^{16}O$ surfaces. The low apparent activation energies are believed to result from adsorbed intermediates, whereas the high values may involve the formation of a singlet O_2 transient. It is shown that eventually the self-diffusion of oxygen ions in the bulk becomes the rate-determining step in the isotope-exchange reaction. Apparent activation energies are determined, and the values are found to depend on surface treatment, (i.e., 44 kcal/mol under reducing and 78 kcal/mol under oxidizing conditions). The involvement of oxygen vacancies under reducing conditions is discussed.

1. Introduction

Mechanistic studies of chemical and physical processes at surfaces of alkaline earth oxides have led to an increased understanding of the reduction of NO by CO, H_2, and hydrocarbons and the oxidative coupling of methane over these materials.[1−6] Involvement of lattice oxygens has been suggested through a surface-oxygen abstraction step by the reducing species. This was confirmed by a recent study which investigated the reduction and reoxidation of CaO surfaces by CO and H_2 as reducing agents and NO as oxidant.[7] The production of a CO_2 transient was observed and a correlation was shown between the amount of CO_2 formed and the amount of NO reduced. These processes are understood to involve an intermediate electron accepting capacity, a property enhanced by the presence of alkali metals.[2−6] It has been suggested that semiconductor models[2,3] and models based on F-type centers[4,5] describe the fate of the excess electrons. In the former model, alkali metal ions were introduced to provide impurity levels in the band gap, while in the latter they were introduced to stabilize the F-type centers.

The purpose of the present study is to clarify further the essential properties of the chemically active substrate. This is achieved by isotope-exchange experiments, a commonly employed technique to determine reaction pathways and identify reactive sites. In this work, kinetic parameters are determined for the oxygen-isotope exchange between $^{18}O^{18}O$ and preoxidized or prereduced $Ca^{16}O$ surfaces, and between $C^{16}O$ or $N^{16}O$ and preoxidized $Ca^{18}O$ surfaces. The results for the oxygen-isotope exchange between O_2 and preoxidized CaO surfaces are consistent with the data available in the literature.

Isotope exchange between an O_2 adsorbate and CaO surfaces was studied by Yanagisawa et al.[12,13] The authors suggested it occurred by adsorption of an O_2 molecule at an O-vacancy, followed by the formation of a bridging bond with an ^{16}O of the CaO surface. No activation energy for the oxygen-isotope exchange was reported here, but a value can be calculated from the work of Cunningham and Healy.[14] An Arrhenius plot based on the initial reaction rates for heterophase oxygen-isotope exchange on powders, outgassed at different temperatures, predicted apparent activation energies of about 12 kcal/mol. The authors proposed a mechanism on the basis of an exchange with hydroxyl groups as the most likely pathway for heterophase isotope exchange at 623 K. Mechanisms for oxygen-isotope exchange based on adsorption have also been suggested for CO and NO as probe molecules. Huzimura et al.[8] investigated the isotopic exchange of oxygen between a CO adsorbate and a MgO surface at temperatures between 100 and 800 K. Proof of the CO bond breakage was provided at temperatures as low as 200 K. This is rather surprising considering the high binding energy in a CO molecule (about 11 eV). A mechanism was proposed on the basis of CO molecules being trapped on low coordinated surface-oxygen sites. The oxygen atom of the CO molecule was suggested to enter into an oxygen vacancy. This understanding implies an adsorbed intermediate and the oxygen exchange to be a concerted reaction driven by thermal heat. Support for this understanding is found in several infrared spectroscopy studies which report a significant number of CO species adsorbed on alkaline earth oxides at temperatures between 77 and 300 K.[9−11] The results presented by Yanagisawa,[15] who studied the NO interaction with thermally activated CaO and SrO surfaces using a temperature-programmed desorption technique, confirm the importance of adsorbed species in the isotopic exchange of oxygen. Adsorbed NO species were observed at temperatures as high as 773 K, and three different sites for oxygen-isotope exchange were proposed. Infrared spectroscopy was used to detect adsorbed NO molecules at temperatures between 40 and 298 K,[16] and adsorptions on both lattice oxygens and cations were suggested.

* Corresponding author: tel, + 46 (0)31 772 28 86; fax, + 46 (0)31 772 28 53; e-mail, filip@inoc.chalmers.se.

S1089-5647(98)01191-2 CCC: $15.00
Published on Web 06/11/1998

Chang et al.[17] studied the oxygen-isotope exchange between gas-phase molecular oxygen and Li-doped MgO lattice oxygens in an attempt to characterize the reactive sites for the oxidative coupling of methane. The amount of oxygen exchanged corresponded to approximately 20 atomic layers. Similar amounts were observed by Peil et al.[18] The exchange reaction became dependent on the self-diffusion of oxygen in the bulk. Measuring the isotope exchange at different temperatures allowed them to determine the apparent activation energy for this process (i.e., 63.5 kcal/mol for a MgO bulk).[19] This apparent activation energy falls in the range, 30−85 kcal/mol, as reported in the literature for temperatures below 1300 °C.[20,21]

The present work reports the effects of surface pretreatment on the apparent activation energy for single-oxygen-isotope exchange between O_2 and CaO. Surface preoxidation resulted in a significantly higher apparent activation energy than for prereduced CaO. Comparisons of the apparent activation energies for oxygen-isotope exchange between $C^{16}O$ or $N^{16}O$ and preoxidized $Ca^{18}O$ surfaces will be made. The asymptotic features in the latter studies are exploited to determine the apparent activation energy for self-diffusion of bulk oxygen.

2. Experimental Section

A fixed bed reactor connected to a quadropole mass spectrometer (QMG 421C-3 of Balzers) was used for the experiments. The quartz reactor (i.d. 22 mm, length 500 mm) had an asymmetric construction to avoid heating the upper metal fitting and the vacuum tight Viton O-ring. Gas sampling was carried out 2 mm under the bed-supporting sintered quartz filter, using a quartz capillary. The temperature was measured 3 mm under the capillary tip with a K-type thermocouple. This position of the thermocouple avoids any interference in the results due to its catalytic activity. The temperature was controlled with a second K-type thermocouple in contact with the heating coil and connected to a Eurotherm temperature controller.

The bed material investigated consisted of 0.250 g CaO (Fisher Scientific) mixed with 1.000 g of quartz sand, pro analysi (Merck). The quartz sand was added to reduce the pressure drop in the bed. The bed was calcined at 1073 K in an Ar flow until adsorbed CO_2 and H_2O species were evacuated (after about 1 h), and the bed was then alternatively exposed to $^{18}O^{18}O$ and $C^{16}O$ or $N^{16}O$. The reaction products, $^{16}O^{18}O$, $^{16}O^{16}O$, $C^{18}O$, $C^{18}O^{16}O$, $C^{18}O^{18}O$, and $N^{18}O$, formed during the experiments, were analyzed by means of a mass spectrometer. A labeled oxide film, $Ca^{18}O$, was formed during exposure of the initial $Ca^{16}O$ material to $^{18}O^{18}O$ at 1073 K, enabling investigations of the temperature dependence on the oxygen exchange between CO or NO and $Ca^{18}O$. This initial step was repeated after every exposure to CO or NO in order to obtain constant surface and bulk properties. The same procedure was followed after exposure of the $Ca^{16}O$ surface to $^{18}O^{18}O$ at different temperatures. An intermediate exposure to CO or NO (reduced or oxidized surfaces respectively) at 1073 K was done in order to obtain a similar $Ca^{16}O$ material before each $^{18}O^{18}O$ exposure. The kinetics of the respective isotope-exchange reactions were determined by evaluating the initial exchange rate constants for different temperatures in Arrhenius plots.

The gases used were 5000 ppm NO, 5000 ppm CO, both in Ar, and 98 atom % $^{18}O^{18}O$. The gases were mixed with pure Ar, using mass flow controllers (series 5800 of Brooks), to a flow of about 25 mL/min and concentrations of about 2500 ppm for CO and NO, and 7200 ppm for $^{18}O^{18}O$. The background due to Ar on the *m*/*e* signal 36 of the mass spectrometer was subtracted for all experiments.

3. Results

The initial rate of oxygen-isotope exchange will be shown to be controlled by the actual isotope-exchange reaction. Once the outermost oxygen layers of the CaO have been exchanged, the rate becomes controlled by the self-diffusion of oxygen ions in the CaO bulk. Results for the oxygen-isotope-exchange reactions are presented for the complete investigated time interval and subsequently used to determine apparent activation energies for the isotope-exchange reactions and the self-diffusion of oxygen.

3.1. Oxygen Isotope-Exchange Experiments. The following reactions were studied:

$$^{18}O^{18}O + {}^{16}O_s \leftrightarrow {}^{18}O^{16}O + {}^{18}O_s \qquad (R_{1a})$$

$$^{18}O^{18}O + 2{}^{16}O_s \leftrightarrow {}^{16}O^{16}O + 2{}^{18}O_s \qquad (R_{1b})$$

$$N^{16}O + {}^{18}O_s \leftrightarrow N^{18}O + {}^{16}O_s \qquad (R_2)$$

$$C^{16}O + {}^{18}O_s \leftrightarrow C^{18}O + {}^{16}O_s \qquad (R_3)$$

The subscript s indicates a surface oxygen. Reactions R_{1a} and R_{1b} describe the oxygen isotope exchange between $^{18}O^{18}O$ and prereduced or preoxidized $Ca^{16}O$ surfaces (section 3.1.1), and R_2 and R_3 describe the oxygen-isotope exchange reactions between $Ca^{18}O$ surfaces and $N^{16}O$ or $C^{16}O$ (section 3.1.2).

3.1.1. Isotope Exchange between $^{18}O^{18}O$ and Preoxidized or Prereduced $Ca^{16}O$. The dependence of the surface pretreatment on the isotope exchange between $^{18}O^{18}O$ and $Ca^{16}O$ surfaces was investigated, taking into consideration both oxidizing and reducing conditions. *Preoxidized surfaces* were obtained after repeated intermediate exposure of the surface to $N^{16}O$ at 1073 K for 45 min. Figures 1a and b show, for temperatures between 706 and 873 K, the oxygen-isotope exchange between $^{18}O^{18}O$ and these surfaces. Figure 1a shows the $^{16}O^{16}O$ production, corresponding to the double-exchanged oxygen (reaction R_{1b}). An initial increase in $^{16}O^{16}O$ concentration is observed for all three temperatures tested. The initial slopes increase with increasing temperature. A distinct maximum can be observed for the double-exchange reaction, becoming even more pronounced with increasing temperature. The qualitative effects were similar for the single-oxygen exchange (reaction R_{1a}, Figure 1b). Characteristic differences between single and double exchange are the significantly larger amounts of single-exchanged oxygen and the systematically higher initial slopes for the single-exchanged oxygen production. Both figures include the feed signal for the $^{18}O^{18}O$ concentration as a measure of the time delay due to the experimental set up.

Oxygen isotope exchange between *prereduced CaO* surfaces and O_2 was also investigated. Reduced surfaces were obtained by repeated intermediate exposure of the surface to $C^{16}O$ at 1073 K for 45 min. A transient CO_2 formation, containing all three isotopes ($C^{18}O^{18}O$, $C^{16}O^{18}O$, and $C^{16}O^{16}O$), was observed during the initial CO exposure. Figures 2a and b show the results of the oxygen-isotope exchange for temperatures between 668 and 817 K. The single-oxygen-exchange reaction (reaction R_{1a}) highlights the main difference between the exchange reactions over preoxidized and prereduced surfaces (i.e., the initial slope in the $^{16}O^{18}O$ concentration is independent of temperature). The temperature effect on the double-oxygen exchange (reaction R_{1b}) over prereduced surfaces is similar to that for preoxidized

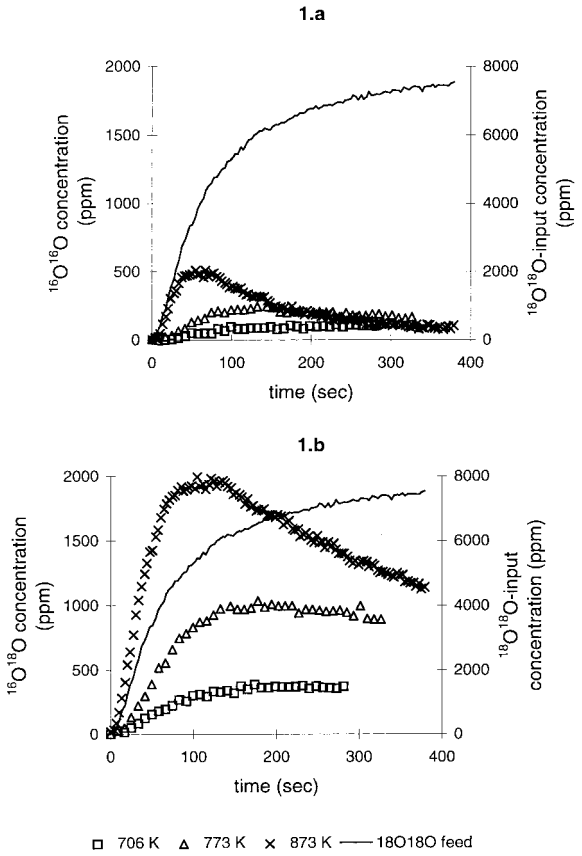

Figure 1. Oxygen-isotope exchange between $^{18}O^{18}O$ and preoxidized $Ca^{16}O$ surfaces at 706, 773, and 873 K. The mass spectrometer *m*/*e* signals 32 ($^{16}O^{16}O$) and 34 ($^{16}O^{18}O$) are shown in a and b, respectively.

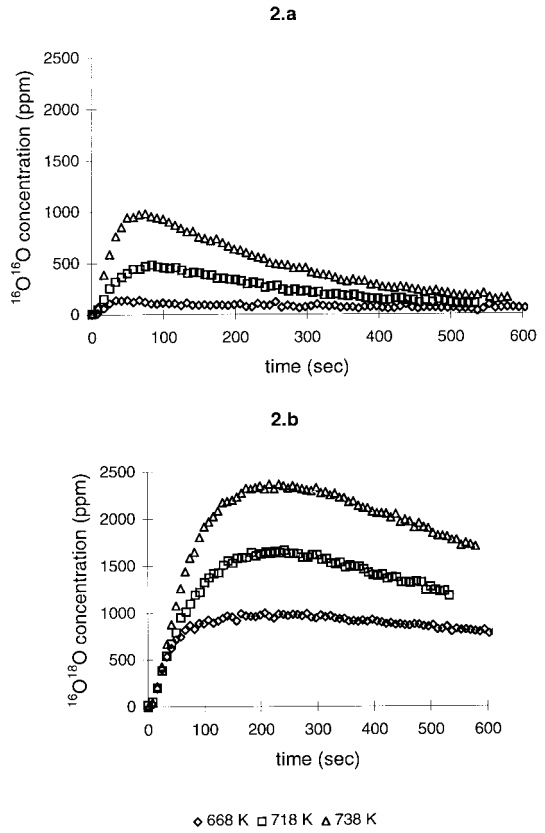

Figure 2. Oxygen-isotope exchange between $^{18}O^{18}O$ and prereduced $Ca^{16}O$ surfaces at 668, 718, and 738 K. The mass spectrometer *m*/*e* signals 32 ($^{16}O^{16}O$) and 34 ($^{16}O^{18}O$) are shown in a and b, respectively.

surfaces (i.e., a temperature-dependent initial slope and an increase in the maximum $^{16}O^{16}O$ formation with increasing temperatures).

3.1.2. Oxygen Isotope Exchange between $Ca^{18}O$ and $N^{16}O$ or $C^{16}O$. CaO surfaces were alternately exposed to $^{18}O^{18}O$ at 1073 K for 15 min and to $N^{16}O$ at temperatures between 573 and 1073 K. This treatment resulted in a fully oxidized material at all times. The oxygen-18 treatment was carried out in order to label the oxygens in the CaO matrix. An ^{18}O concentration gradient from the surface into the bulk can be expected. Oxygen-isotope exchange between the labeled $Ca^{18}O$ surface and $N^{16}O$ (reaction R_2) was observed for all tested temperatures. Figure 3 shows both the isotope exchanged $N^{18}O$ and the $N^{16}O$ feed concentrations. The initial slope in $N^{18}O$ concentration was independent of temperature, whereas the maximum in $N^{18}O$ production increased with increasing temperature. The $N^{16}O$ feed is also included in Figure 3 to give an indication of the response time of the experimental set up.

The above experiment with NO was repeated, replacing NO with CO. Figure 4 shows the oxygen isotope exchange between $C^{16}O$ and $Ca^{18}O$ (reaction R_3). Similar results as for the $N^{16}O$/$Ca^{18}O$ system were obtained (i.e., the amount of oxygens exchanged are a function of temperature), whereas the initial slopes were insensitive to temperature. The decreasing part of the $C^{18}O$ and $N^{18}O$ concentration curves (Figures 3 and 4) are discussed in detail under section 3.2.2, where modeling of oxygen self-diffusion was attempted.

3.2. Apparent Activation Energies. *3.2.1. Apparent Activation Energies for Oxygen Isotope Exchange.* The mass balances for reactions R_{1a}, R_{1b}, and R_2 over preoxidized CaO surfaces are straightforward. The loss of reactant corresponded to the amount of isotope exchanged molecules formed in accord

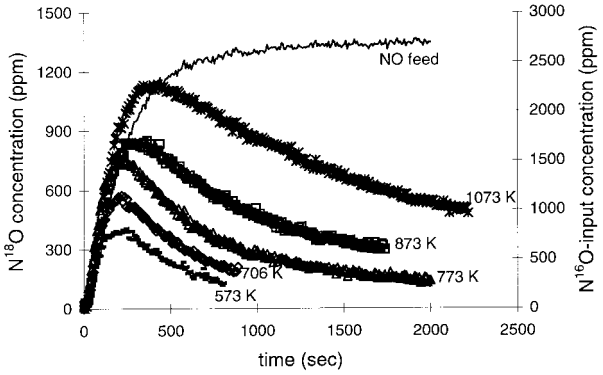

Figure 3. Oxygen-isotope exchange between $N^{16}O$ and a $Ca^{18}O$ surface investigated in the temperature range 573−1073 K.

with the relations

$$[N^{16}O^{f}] - [N^{16}O] = [N^{18}O]$$

and

$$[^{18}O^{18}O^{f}] - [^{18}O^{18}O] = [^{18}O^{16}O] + [^{16}O^{16}O]$$

where f stands for feed conditions. The single (R_{1a}) and double (R_{1b}) oxygen isotope exchange between $^{18}O^{18}O$ and prereduced surfaces are, however, affected by an initial reoxidation. This loss of $^{18}O^{18}O$ was compensated for in the analysis by taking the sum of all O_2 species as the feed (i.e., $[^{18}O^{18}O] + [^{18}O^{16}O] + [^{16}O^{16}O]$). Similarly, an initial loss was also observed for CO, since CO reduced the surface by forming CO_2. This effect was again accounted for in the mass balance for reaction R_3 by taking the sum of $[C^{16}O]$ and $[C^{18}O]$ as the $C^{16}O$ feed concentration, $[C^{16}O^{f}]$.

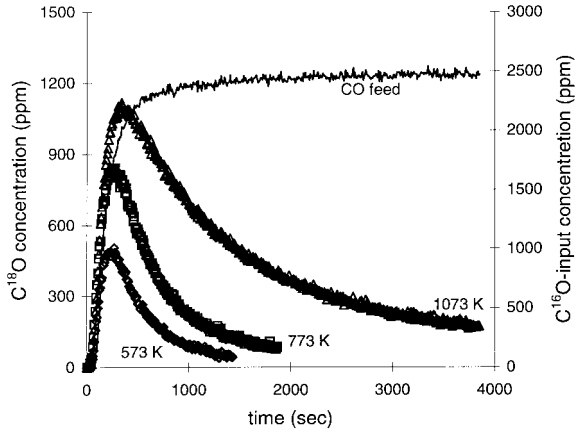

Figure 4. Oxygen-isotope exchange between $C^{16}O$ and a $Ca^{18}O$ surface at 573, 773, and 1073 K.

The apparent activation energies for the actual isotope exchange can be determined from the initial slopes in a concentration−time diagram. Rate constants were computed assuming a second-order reaction proportional to $[NO/CO/O_2]\cdot[O_s]$ where $[O_s]$ is the concentration of $^{16}O_s$ for reactions R_{1a} and R_{1b} and $^{18}O_s$ for reactions R_2 and R_3. The surface-oxygen concentration was treated as a constant as long as the slope remained constant. The above assumption of a pseudo-first-order reaction is similar to the one proposed by Lizuka et al.[22] and was shown to be efficient in the interpretation of the oxygen-isotope exchange between CO_2 and MoO_3. The rate constant was evaluated by solving the material balance, treating the reactor as an integral reactor

$$k = (F/(C_{tot}\, C_{Os} W)) \ln(y^f/y) \qquad (1)$$

where F is the molecular flow, C_{tot} the total concentration, C_{Os} the surface-oxygen concentration, W the amount of catalyst, and y the molar ratios of the respective species tested. The surface-oxygen concentration was estimated by treating the CaO grains as cubes with a total surface area of 0.9 m^2 (determined by BET). Evaluations of the rate constants in Arrhenius plots for oxygen-isotope exchange between $^{18}O^{18}O$ and $Ca^{16}O$ and between $N^{16}O$ or $C^{16}O$ and $Ca^{18}O$ are made in Figure 5a and b, respectively. Apparent activation energies and preexponential factors for the respective reactions are collected in Table 1.

Apparent activation energies in two significantly different ranges were found. Low values are seen for the oxygen-isotope exchange between $C^{16}O$ or $N^{16}O$ and the $Ca^{18}O$ surfaces, as well as for single-oxygen-isotope exchange between $^{18}O^{18}O$ and prereduced $Ca^{16}O$ surfaces. This is contrasted by double-oxygen-isotope exchange over prereduced $Ca^{16}O$ surfaces and both single- and double-oxygen-isotope exchange over preoxidized surfaces. Apparent activation energies of about 17 kcal/mol are observed for these. Note also the effects on the preexponential factor. The value for single-oxygen-isotope exchange over preoxidized surfaces was about twice as large as that for the double exchange. Prereduction of the surface resulted in an increased preexponential factor for the double-oxygen-isotope exchange reaction. This trend can also be observed from the relative positions of the straight lines in the Arrhenius plots (Figure 5a). No significant difference was observed between NO and CO (Figure 5b).

3.2.2. Apparent Activation Energies for Self-Diffusion of Oxygen: A Model. The concentration profile of ^{16}O in the bulk of $Ca^{18}O$, as well as of ^{18}O in the bulk of $Ca^{16}O$, are functions of the distance to the surface (x) and time. Solving Fick's

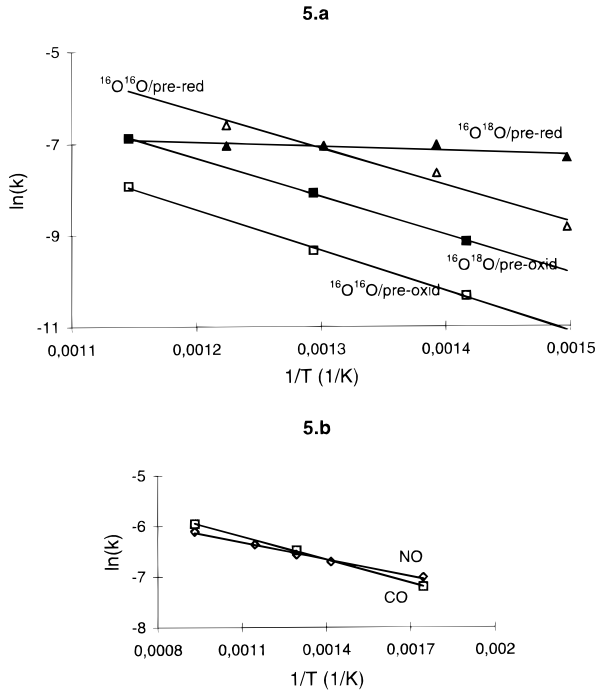

Figure 5. Arrhenius plots for the oxygen-isotope exchange for (a) single- and double-oxygen-isotope exchange between $^{18}O^{18}O$ and both prereduced and preoxidized $Ca^{16}O$ surfaces and (b) oxygen exchange between $N^{16}O$ or $C^{16}O$ and $Ca^{18}O$ surfaces.

TABLE 1: Apparent Activation Energies (E_a) and Preexponential Factors (A) for the Examined Isotope-Exchange Reactions

	E_a (kcal/mol)	A
O_2		
single exchange		
preoxidized	16.6	15.1
prereduced	1.8	2.8×10^{-3}
double exchange		
preoxidized	17.7	9.5
prereduced	16.1	30.4
NO	2.2	6.1×10^{-3}
CO	3.0	1.1×10^{-2}

second law for a semi-infinite body and constant partial pressures of $^{16}O/^{18}O$ at the gas-solid interphase produces[23]

$$C(x,t) = C_s \,\mathrm{erfc}[x(4Dt)^{-1/2}] \qquad (2)$$

where C_s is the surface-oxygen concentration in mol/m^3 and D is the intrinsic diffusivity expressed in m^2/s. After a certain time, depending on probe molecule and temperature, the oxygen-isotope exchange rate is determined by the rate of self-diffusion of $^{18}O/^{16}O$ from the bulk to the surface, or equivalently, of $^{16}O/^{18}O$ transport from the surface into the bulk. At a certain time and for a certain position, the atomic flux in the bulk becomes a function of the concentration gradient as described by Fick's first law:

$$J(x,t) = -D\, \mathrm{d}C(x,t)/\mathrm{d}x \qquad (3)$$

where J is the flux of oxygen ions (mol/m^2 s), D the diffusivity, and C the concentration as defined in eq 2. Differentiation of eq 2, and calculating the flux J according to eq 3 at the surface, for t sufficiently large gives

$$J(0,t) = C_s\, (2/\pi^{1/2}) 1/(4Dt)^{1/2} \qquad (4)$$

where $C_s\, (2/\pi^{1/2})$ has a value of 0.112 mol/m^3.

TABLE 2: Values for the Parameters α, β, α_1, β_1, and γ for the Functions Describing the Oxygen Isotope Exchange for NO (Eq 5) and CO (Eq 6) as Probe Molecules

temperature (K)	NO and CO		$CO_{initially}$		
	α	β	α_1	β_1	γ
573	10 129	−227.35	16 610	−437.53	1.9357×10^{-6}
706	14 161	−287.71			
773	17 030	−253.25	25 183	−574.51	1.891×10^{-7}
873	22 308	−238.96			
1073	33 175	−197.91	33 489	−380.13	1.2236×10^{-9}
E_a (kcal/mol)	74.3			44.9	

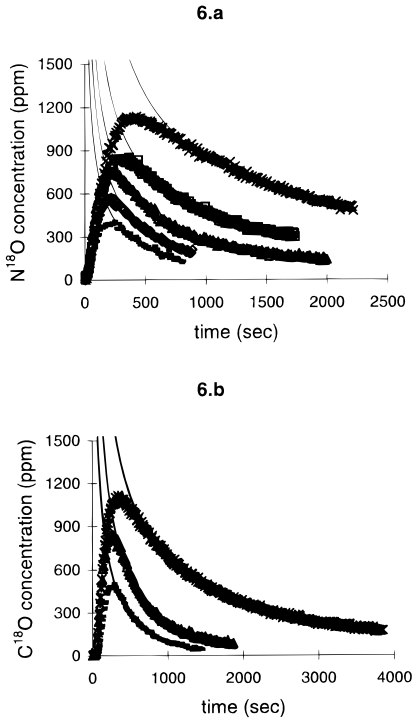

Figure 6. Comparison between the employed model for the self-diffusion of oxygen and the experimental points for (a) isotope exchange between $N^{16}O$ and a $Ca^{18}O$ surface and (b) isotope exchange between $C^{16}O$ and a $Ca^{18}O$ surface in the temperature range 573 and 1073 K.

Modeling the decline in the oxygen-isotope-exchange curves for NO as the probe molecule was made by optimizing the constants α and β in relation 5 by the least-squares method

$$J(0,t) \approx (\alpha/t^{1/2}) + \beta^{1/2} \quad (5)$$

The parameter α is proportional to the inverse of the square root of the diffusivity as seen by comparing eq 4 and 5. The parameter β was introduced to account for deviations from the idealized model (i.e., a semi-infinite substrate is assumed rather than grains) as well as the fact that not all oxygens in the bulk are isotopically labeled. The applicability of eq 5 rests on the understanding of the oxygen distribution in the substrate being 100% ^{18}O at the surface, 100% ^{16}O in the core, and a concentration gradient in between. The model applies as long as this gradient is negligible, meaning that a thin layer in the vicinity of the surface is probed. Particularly, β is understood to be a sensitive function of the residual ^{16}O activity. Table 2 gives the values for the parameters α and β for different temperatures. The temperature dependence of the diffusivity is described by an Arrhenius equation and the relation between α and the diffusivity is used to evaluate the activation energy for self-diffusion of oxygen. Figure 6a shows the result of the modeling: good agreement with the experimental data points is obtained.

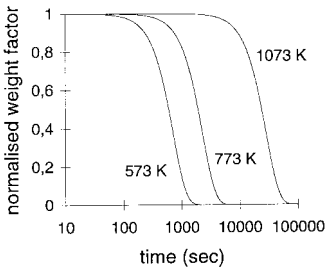

Figure 7. The effect of temperature on the shape of the normalized weight function.

Contrary to the case of NO, no acceptable fit to the simple model could be obtained for CO as the probe molecule. This is not surprising as exposure of the preoxidized surface to CO has been shown to result in surface-oxygen abstraction and formation of vacancies. Initially, the self-diffusion of oxygen should be controlled by a vacancy-induced mechanism, which is expected to have a substantially lower activation energy than in fully oxidized substrates. Even for a diffusion mechanism involving vacancies, Fick's laws should be obeyed and proportionality of J to $t^{-1/2}$ should prevail. Eventually, the vacancies are expected to have diffused into the bulk and the self-diffusion of oxygen will be similar to that found for NO as the probe molecule. Therefore, the tails of the oxygen-isotope exchange curves should be modeled by a sum of two functions, each of the form 5, and weighted according to

$$J(0,t) = [\exp(-\gamma\, t^2)J_1(0,t)] + [(1 - \exp(-\gamma t^2))J_2(0,t)] \quad (6)$$

where

$$J_1(0,t) \approx \alpha_1/t^{1/2} + \beta_1$$

$$J_2(0,t) \approx \alpha/t^{1/2} + \beta$$

where α and β are the parameters obtained for the NO case at the corresponding temperatures and γ determines weight factors which are optimized together with the parameters α_1 and β_1 by the least-squares method. See Table 2 for the fitted values of the parameters and Figure 6b for the result of the modeling.

The values of α increase with increasing temperature. Calculating the diffusivities at the temperatures tested and plotting these in an Arrhenius plot produces an apparent activation energy of 74.3 kcal/mol when NO is used as the probe molecule. The diffusivity as determined with CO is initially enhanced by the presence of vacancies, consistent with a lower apparent activation energy, 44.9 kcal/mol. This enhanced oxygen transport affects β since it is determined by the residual activity of ^{16}O. In Figure 7 the normalization factor is plotted as a function of time for the three temperatures investigated. The importance of this factor decreases with increasing temperatures. At 1073 K, α and α_1 are approximately equal, whereas significantly more pronounced differences were found at the lower temperatures.

4. Discussion

The CaO catalyst can be divided into three regions comprising *the physical surface* where the exchange between the gas phase and the solid occurs, *several subsurface layers* readily available for exchange, and *the bulk oxide*.[19] This partitioning is used in the present study, where kinetic parameters for surface-oxygen exchange and self-diffusion of oxygen in the bulk are investigated by means of isotopic labeling. Oxygen-exchange rates

between the physical surface and probe molecules revealed information concerning the actual isotope-exchange reaction. Apparent activation energies for single- and double-oxygen-isotope exchange between $^{18}O^{18}O$ and preoxidized or prereduced $Ca^{16}O$ surfaces and oxygen exchange between $C^{16}O$ or $N^{16}O$ and preoxidized $Ca^{18}O$ surfaces were determined and are discussed in section 4.1. An increase in temperature resulted in an increased involvement of the subsurface oxygens in the isotope-exchange reaction. The bulk oxygens gradually become more important, resulting in an asymptotic exchange rate controlled by the self-diffusion of oxygen through the bulk. Effects of reduction and oxidation on apparent activation energies of self-diffusion of oxygen were demonstrated and are discussed in section 4.2.

4.1. Oxygen Isotope Exchange. The apparent activation energies for oxygen isotope exchange (Table 1) are consistent with the values reported in the literature. Observations of two distinct classes of apparent activation energies for isotope exchange have been discussed previously for exchange between an ionic solid MX and the corresponding diatomic gas X_2.[24] Winter[25] suggested the involvement of F-type centers in the isotope exchange reactions that correspond to the lower apparent activation energies. However, the higher values are not well understood. No correlation with electronic properties of the materials was observed.[25] The higher apparent activation energies obtained in this work for the single- and double-oxygen exchange between O_2 and a preoxidized CaO surface, as well as the double-oxygen exchange between O_2 and a prereduced CaO surface, were similar to estimations from the initial rates of oxygen-isotope exchange between O_2 and CaO as calculated from the results of Cunningham and Healy.[14] These values were contrasted by the low apparent activation energy observed in the present study for single-oxygen-isotope exchange between O_2 and prereduced CaO surfaces. The magnitude of the latter is comparable to those obtained for oxygen exchange between CO or NO and CaO surfaces. Exposure of a CaO surface to a reducing agent at elevated temperatures has been shown to result in the formation of reactive sites, as a direct consequence of the surface-oxygen abstraction step.[7] The promoting effect of F-type centers has been demonstrated for the oxygen exchange over zinc oxide and other metal oxides[26,27] and can be expected to cause the drastic reduction in the apparent activation energy for the single-oxygen-isotope exchange over prereduced surfaces observed in the present study. The high apparent activation energy for double-oxygen exchange over prereduced surfaces suggested that the reoxidation of the surface is a fast process.

The oxygen-isotope exchange between $C^{16}O$ and $Ca^{18}O$ surfaces could involve similar sites as the $^{18}O^{18}O$ single-oxygen exchange with a prereduced $Ca^{16}O$ surface, since exposure of CaO to CO resulted in a surface-oxygen abstraction.[7] However, the amount of surface oxygens abstracted is low at temperatures below 773 K, which makes a mechanism based on adsorbates such as CO_2^-, CO_2^{2-}, and CO_3^{2-} more likely. The former was observed using electron spin resonance,[28] whereas the latter two are among the many species suggested by IR spectroscopy data.[9−11] Further evidence for a mechanism based on adsorption for CO is found in the similarity with NO at elevated temperatures, since for the latter a fully oxidized surface is obtained at all times. Yanagisawa suggested that NO was adsorbed as NO_2^- or NO_3^-.[15] Necessary for these intermediates is the presence of O^- sites, and the existence of such finds support in the pretreatment of the oxide (i.e., 7500 ppm O_2 at 1073 K). The similarity between CO and NO as probe molecules, seen in the present study, makes the involvement of reduced sites unlikely in the exchange reactions with these molecules. Previous results from thermal desorption gas analysis are consistent with this understanding. It was shown that CO, NO, and O_2 desorb at temperatures up to about 1000 K.[8,12,15] Thus, the first factor controlling the isotope exchange is the availability of adsorption sites. The physical origin of the 17 kcal/mol apparent activation energy remains unsolved. This value is only obtained for oxygen exchange including an O_2 molecule and may be ascribed to an inherent property of this molecule upon adsorption. The singlet−triplet splitting in O_2 is such a feature.[29] It is reasonable to expect such a property to be effective in the entrance channel of the exchange process (i.e., an $^3O_2$ to $^1O_2$ conversion is necessary for oxygen exchange). This constraint is not present for NO and CO and consequently different apparent activation energies for oxygen exchange were observed. The presence of excess electrons, resulting from the prereduction treatment, makes the $^2O_2$ adsorption channel accessible for single-oxygen exchange between O_2 and prereduced CaO surfaces, and consequently the lower apparent activation energy was observed.

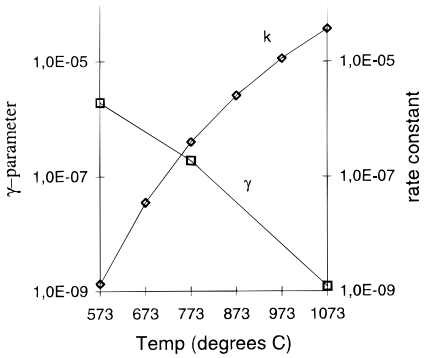

Figure 8. Relation between the γ-parameter in the normalized weight function and the rate constant k for the surface-oxygen abstraction.

4.2. Self-Diffusion of Oxygen. A straightforward understanding of the oxygen self-diffusion emerges from the NO study, and an apparent activation energy of 74.3 kcal/mol is obtained. A similar value, 63.5 kcal/mol, was determined for MgO.[19] Determination of the apparent activation energy for oxygen self-diffusion using CO is more complicated. A surface-oxygen abstraction step upon CO exposure introduces vacancies in the surface layer of the material. Despite the necessity of a temperature of about 773 K to obtain reasonable CO_2 production, even at 573 K some surface oxygens are expected to be removed. In previous work, the temperature dependence of the rate constant for surface-oxygen abstraction was determined,[7] and this temperature dependence is shown in Figure 8. The temperature dependence of the γ parameter, which determines the weight function, is also included in Figure 8 (see section 3.2.2). For 573 K, a low rate constant and a high γ value were observed. This implies an initial dominating mechanism based on vacancies introduced by the surface-oxygen abstraction. With time, the vacancies diffused into the bulk and a similar mechanism as for NO as the probe molecule is expected to become dominant. Increased temperature results in an increased rate constant for surface-oxygen abstraction and the importance of the vacancy-controlled mechanism diminishes. The experiment at 1073 K confirms this trend. Note the very small effect of the weighing at this temperature, as seen by comparing the parameters α and α_1. This is expected due to the small number of vacancies in the vicinity of the surface, and consequently the bulk property prevails at these elevated temperatures.

5. Concluding Remarks

Discriminating molecular properties that control adsorption are of interests in order to achieve high selectivity in the NO_x reduction activity of catalysts. The present study has focused on some relevant molecules, choosing CaO as a model substrate. The rates of oxygen-isotope exchange between CO, NO or O_2, and CaO surfaces were investigated in a comparative study and were shown to be initially controlled by the actual isotope-exchange reaction. After this first stage, the rate was found to depend increasingly on the rate of self-diffusion of oxygen in the CaO bulk.

The higher apparent activation energies for the actual exchange process were speculated to be consequences of the singlet−triplet spectroscopy of molecular oxygen. A comparison of the preexponential factors for the single- and double-oxygen exchange between O_2 and *preoxidized* CaO surfaces suggested that the double-exchange reaction consists of two successive single-exchange reactions. The apparent activation energy for self-diffusion of oxygen was determined with NO as the probe molecule. The temperature dependence of the diffusivity was exploited and 74 kcal/mol was obtained for fully oxidized CaO at all times. To understand the results for CO as the probe molecule, the diffusion-controlled time domain was divided into early and late subdomains. The early part was controlled by the transient dynamics of oxygen vacancies, the presence of which lowered the apparent activation energy, and an estimated value of about 45 kcal/mol was obtained.

Acknowledgment. The authors are in debt to the Swedish National Board for Industrial and Technical Development for financial support (NUTEK).

References and Notes

(1) Ito, T.; Lunsford, J. H. *Nature* **1985**, *314*, 721.
(2) Shi, C.; Xu, M.; Rosynek, P.; Lunsford, J. H. *J. Phys. Chem.* **1993**, *97*, 216.
(3) Lin, C.-H.; Wang, J.-X.; Lunsford, J. H. *J. Catal.* **1988**, *111*, 302.
(4) Wu, M.-C.; Truong, C. M.; Goodman, D. W. *Phys. Rev. B* **1992**, *46*, *12*, 688.
(5) Wu, M.-C.; Truong, C. M.; Coulter, K.; Goodman, D. W. *J. Catal*. **1993**, *140*, 344.
(6) Zhang, X.; Walters, A. B.; Vannic, M. A. *J. Catal*..; **1994**, *146*, 568.
(7) Acke, F.; Panas, I.; Strömberg, D. *J. Phys. Chem.* **1997**, *101*, 6484.
(8) Huzimura, R.; Yanagisawa, Y.; Matsumura, K.; Yamabe, S. *Phys. Rev. B*, **1990**, *41*, 3786.
(9) Coluccia, S.; Garrone, E.; Guglielminotti, E.; Zecchina, A. *J. Chem. Soc., Faraday Trans. 1* **1981**, *77*, 1063.
(10) Garrone, E.; Zecchina, A.; Stone F. S. *J. Chem. Soc., Faraday Trans. 1* **1988**, *84*, 2843.
(11) Babaeva, M. A.; Bystrov, D. S.; Kovalgin, A. Y.; Tsyganeneko, A. A. *J. Catal.* **1990**, *123*, 396.
(12) Yanagisawa, Y.; Yamabe, S.; Matsumura, K.; Huzimura, R. *Phys. Rev. B*, **1993**, *48*, 4925.
(13) Yanagisawa, Y.; Huzimura, R.; Matsumura, K.; Yamabe, S. *Surf. Sci.* **1991**, *242*, 513.
(14) Cunningham, J.; Healy, C. P. *J. Chem. Soc., Faraday Trans. 1*, **1987**, *83*, 2973.
(15) Yanagisawa, Y. *Appl. Surf. Sci.* **1996**, *100/101*, 256.
(16) Platero, E. E.; Spoto, G.; Zecchina, A. *J. Chem. Soc., Faraday Trans. 1*, **1985**, *81*, 1283.
(17) Chang, Y.-F.; Somorjai, G. A.; Heineman, H. *J. Catal*. **1993**, *142*, 697.
(18) K. P.; Goodwin, J. G., Jr.; Marcelin, G. *J. Phys. Chem*. **1989**, *93*, 7977.
(19) Peil, K. P.; Goodwin, J. G., Jr.; Marcelin, G. *J. Catal*. **1991**, *131*, 143.
(20) Viera, J. M.; Brook, R. J. In: *Structure and Properties of MgO and Al_2O_3 Ceramics*; Kingery, W. D., Ed.; (American Ceramic Society Press: Columbus, OH, 1984; p 438.
(21) Oishi, Y.; Ando, K. In: *Structure and Properties of MgO and Al_2O_3 Ceramics*; Kingery, W. D., Ed.; American Ceramic Society Press: Columbus, OH, 1984; p 463.
(22) Lizuka, Y.; Tanigaki, H.; Sanada, M.; Tsunetoshi, J.; Yamauchi, N.; Arai, S. *J. Chem. Soc., Faraday Trans.* **1994**, *90*, 1307.
(23) Wuensch, B. J.; Steele, W. C.; Vasilos, T. *J. Chem. Phys.* **1973**, *58*, 5258.
(24) Cunningham, J.; Goold, E. L.; Leahy, E. M. *J. Chem. Soc., Faraday Trans. 1* **1979**, *75*, 305.
(25) Winter, E. R. S. *J. Chem. Soc. A* **1968**, 2889.
(26) Shvets, V. A.; Kuznetsov, A. V.; Fenin, V. A.; Kazansky, *J. Chem. Soc., Faraday Trans. 1* **1985**, *81*, 2913.
(27) Cunningham, J.; Goold, E. L.; Leahy, E. M. *J. Chem. Soc., Faraday Trans. 1* **1979**, *75*, 301.
(28) Huzimura, R.; Kurisu, H.; Okuda, T. *Surf. Sci.* **1988**, *197*, 444.
(29) Huber, Herzberg *Construction of Diatomic Molecules*; van Nostrand: New York, 1979.